Fast Neutron Imaging for SNM Detection

Victor Bom

Delft University of Technology
Mekelweg 15, 2629 JB Delft, the Netherlands

Email contact of author: V.R.Bom@TUDelft.nll

Abstract Special Nuclear Materials (SNMs) are difficult to detect because the gamma emissions are weak and the neutron emissions fall below the natural back ground beyond practical stand off distances. The application of direction sensitive imaging techniques to improve the signal to back ground ratio is mandatory for passive as well as active interrogation methods. A fast neutron imaging detector for the detection of SNMs in sea containers is being developed to be applied in the harbor of Rotterdam in cooperation with Customs Rotterdam. The detection principle is based on two subsequent elastic neutron-proton scatterings in one single organic scintillator block that allow to determine the direction cone of the incident neutron. The scintillator material must have a very short decay time because the time difference between the scatter events is in the nanosecond second regime.

1 Introduction

Illegal transport of Special Nuclear Materials (SNMs) is generally regarded as the utmost terrorist risk. A nuclear weapon, however primitive and inefficient, that is set off in a populated area will have an extremely devastating effect, humanitarian, psychological as well as material, with world wide consequences far out reaching those of the 9/11 disaster. Besides a SNM explosion the effect of a 'dirty bomb' pales into significance. Although the chance that a terrorist organization assembles such a weapon may be small the consequences are enormous and can not be overlooked. It is therefore important to be able to check the transport chain for SNMs.

Nuclear materials typically emit gamma rays and fast neutrons, see table 1. The gamma ray intensity emitted by SNMs is small. For example, the ^{40}K present in a container load tiles or broccoli emits over 10 times the amount of gamma rays of one kilo plutonium. The neutron emissions of SNMs are also small.

SNMs can therefore easily be hidden in the transport chain, e.g. in sea containers, with standard detection portals not being able to find such materials. To illustrate this: in 2002 an ABC news reporter made a trip with 10 kg uranium (depleted) through seven countries in 25 days and finally shipped it into the U.S. without being questioned anywhere [1]. Attempts to smuggle or sell SNMs are regularly reported [2–4].

The gamma rays emitted by SNMs are easily shielded because of their generally low energy. The fast neutron emissions are much more difficult to shield properly and are suited for the detection of SNMs.

The neutron background at sea level due to cosmic rays and solar activity shows an energy spectrum with a broad peak between 1 and 10 MeV. The background flux can very roughly be estimated below 10 MeV to be 0.01 $\mathrm{n/s.cm^2}$ [5]. One kilogram of weapon grade plutonium (WGP) [1] emits 6×10^4 n/s (table 1) following a Watt energy spectrum [6]. Simple algebra shows that the neutron flux from the plutonium becomes over shadowed by the background

[1] This amount is sufficient for an explosion four times as powerful as the 9/11 disaster, assuming sufficient technical skill.

SNM	**form**	**Gamma-rays**		**Neutrons**	
		Energy	Intensity	Energy	Intensity
Uranium	Highly enriched	1.001	$\leq 10^4$	≈2	1
		2.6	2.7×10^4		
plutonium	Mixed Oxide	0.769	10^5	≈2	$\approx 5 \times 10^5$
	Weapons grade	0.769	2.3×10^5	≈2	$\approx 6 \times 10^4$
Californium 252					$\approx 2 \times 10^6$

Table I: The spontaneous gamma ray and neutron emissions of uranium and plutonium. Emissions are per kg.s, energies are in MeV. For comparison similar information is shown for 1 microgram of ^{252}Cf.

beyond a distance of about 7 m. Standard scanning methods will not be able to detect such an amount of WGP in a sea container since 7 m is of the order of the dimension of the container. Some background reduction can be achieved by energy discrimination but a more substantial reduction of the background will be possible by using a fast neutron detector with imaging properties. The background rate within an opening angle corresponding to an angular resolution of 10° for example is reduced by a factor:

$$\frac{4\pi}{\pi \tan^2 10^\circ} = 128$$

under the assumption of isotropy of the back ground. With such a direction sensitive detector the WGP can be detected above the natural background up to a distance of about 70 m.

Directional fast neutron detectors are known for some time [7–9]. These devices use multiple scintillators with some intermediate distance to allow for time-of-flight methods to be applied. Limitations exist on the neutron incident directions and on the efficiency and energy and direction resolution. Some of these limitations can be removed or alleviated by using one single large scintillator. This method has become possible because of

- the recent discovery of new types of scintillator materials with an extremely fast sub-nanosecond response,
- the improved quality of fast light sensors, and
- the very recently introduced pulse samplers of 8 giga-samples per second, thus allowing the required sub-nanosecond time resolution.

This paper presents calculations and simulation results for a single scintillator directional sensitive fast neutron detector.

2 Detection principle

Fast neutrons lose energy when traveling through hydro–carbon scintillator materials by interactions with protons and Carbon nuclei. The recoil proton energy is released as scintillator light and the collision kinematics uniquely defines the scattering angle of the neutron. The proton track itself is too short to be observed. When the scattered neutron experiences a second collision with a proton inside the scintillator the direction of the original incoming track can be determined see figure 1.

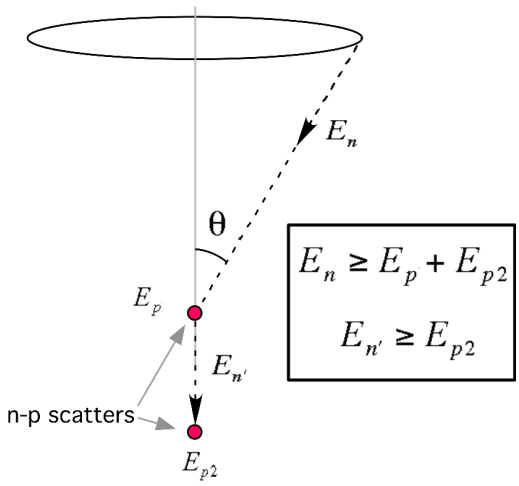

Figure 1: Double elastic n-p scattering showing the basic kinematics of event reconstruction. If the full neutron energy is measured, the incident neutron direction is restricted to the mantle of a cone and an 'event circle' can be drawn.

From the coordinates and time difference of the two interactions, one can determine the direction and the energy $E_{n'}$ of the scattered neutron. The energy of the incident neutron E_n then follows as the sum of this scattered neutron energy and the energy of the first recoil proton E_p as derived from the scintillation light flash. The neutron scatter angle Θ can be derived from the simple kinematics of elastic non–relativistic scattering as:

$$E_n = E_p + E_{n'}$$

$$\sin^2 \Theta = \frac{E_p}{E_n}$$

where E_p and E_n are respectively the kinetic energies of the first recoil proton and of the incident neutron and $E_{n'}$ is the kinetic energy of the neutron after the first scattering. The direction of the incident neutron is situated on the mantle of a cone with

- its top at the position of the first collision,
- its cone angle defined by the scattering angle
- its axis along the neutron path after the first collision

3 The detector

The detector consists of a scintillator block (see figure 2) of $10 \times 10 \times 10$ cm^3 with photomultiplier tubes (PMTs) or other fast-response light sensors mounted on the six sides. The position of the scatter event in the scintillator block, is determined from the light intensity distribution over the PMTs. The time of the collision is determined from the light arrival times at the PMTs. The difference in light arrival times between two opposite cube faces also provides information about the position of the event. A 1 cm displacement in the event position causes a 0.1 ns change in the arrival times difference. Figure 2 shows two cones constructed from this information. If the neutrons originate from the same source, there will be a common direction on the conoids pointing at the source. The intersecting lines of several cones will point in the direction of the source of neutrons.

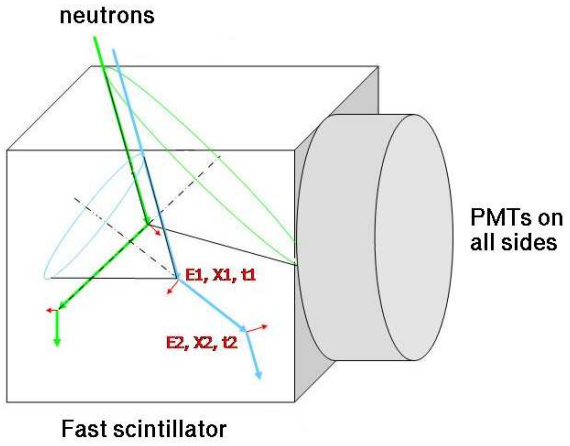

Figure 2: Schematic of the source-imaging fast-neutron detector. Reactions of two incoming neutrons are shown (tracks in green and blue). The small arrows show recoiling protons (in red). For simplicity only one light sensor (PMT) is indicated.

3.1 Angular resolution

The distances and times between the two n–p collisions are of the order of a few centimeters and nanoseconds in common plastic neutron scintillator materials. Accurate construction of the cones requires enough scintillation light per collision and a sub nano–second time resolution.

Figure 3 shows the n–p scatter angle Θ calculation accuracy for 2.5 MeV neutrons assuming energy, position and time 1-σ resolutions of respectively: 16%, 5 mm and 0.4 ns. The drawn black line shows the real scattering angle as function of the proton energy. The blue drawn

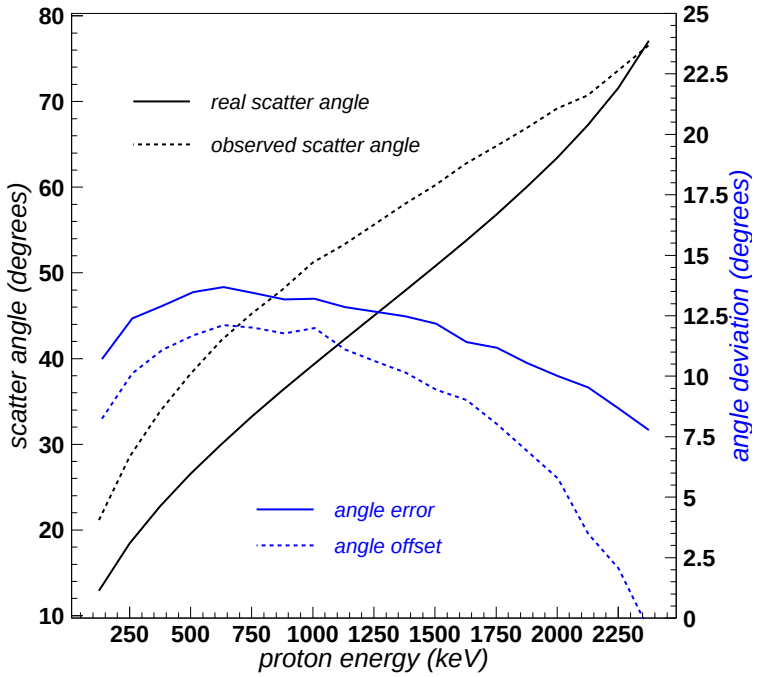

Figure 3: Direction accuracy estimation. Incident neutron energy: 2.5 MeV; recoil proton energy resolution 16 %; position accuracy: 5 mm; time resolution: 0.4 ns

first hit	fraction	second hit	fraction
proton	55%	proton	27%
		carbon-nucleus	28%
carbon-nucleus	32%	proton	
		carbon-nucleus	
no hit	13%		

Table II: Simulation results for the distribution of hit events. Fractions are wit respect to the incident neutron flux. Neutron energy: 2.5 MeV, mono-energetic. Scintillator size: $10 \times 10 \times 10\ cm^3$

line, which refers to the right hand scale, shows the standard deviation error in the calculated scatter angle. Since all proton energies have equally probability in n–p scattering the average error in the scatter angle is around 12°. Scatter events in which the observed distance traveled by the scattered neutron or time difference between the scatter events are below the respective resolutions are disregarded. Also events are disregarded if the observed proton energy falls below 200 keV. The omission of these events results in a difference between the calculated scatter angle and the real one, shown by the dashed curves in the figure. The average of the offset is about 7°.

3.2 Efficiency

The neutron can scatter from a proton or from a carbon-nucleus. When a carbon-nucleus is hit the neutron energy change is small because of the large mass difference. The scintillation light of the carbon ion is too faint to be detected well because the carbon ion acquires only a small energy. The direction change as a result of neutron–carbon-nucleus interactions can therefore not be determined and consequently also the initial neutron direction can not be calculated. The

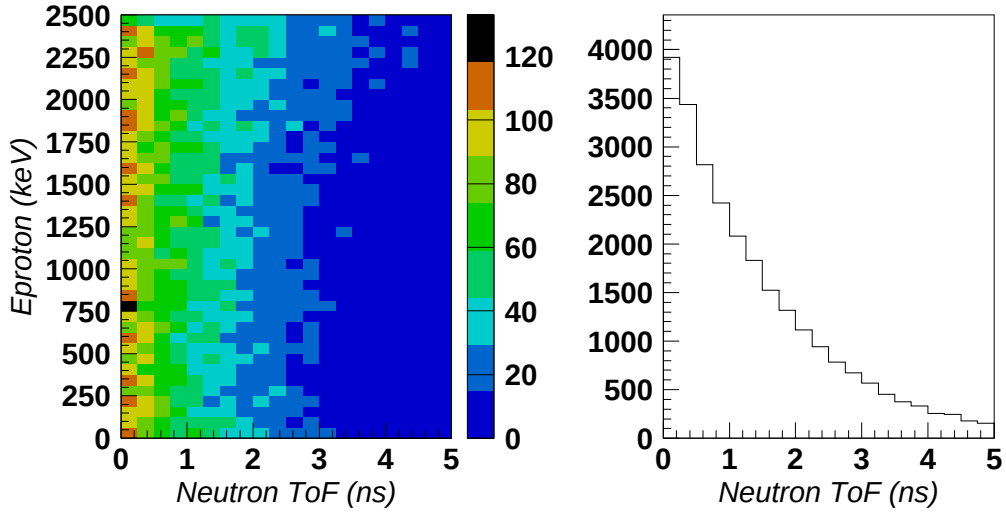

Figure 4: Simulated distribution of events as function of the proton energy and the time-of-flight between two scatter events in a plastic scintillator for 2.5 MeV incident neutrons.

events which allow a calculation of a direction cone thus must have a first and a second hit both with a proton target. Other events give a wrong direction or no direction at all. Table II shows the results of simulations for the hit distribution of 2.5 MeV neutrons incident on a $10 \times 10 \times 10\,\mathrm{cm}^3$ scintillator. About 27% result in 'good' events. The other 73% will contribute to the background and will be distributed over 4π steradians.

Among the 27% good events some can not lead to a proper cone construction because the time difference or the E_p is too small. Figure 4 shows the results of a simulation of the penetration of 2.5 MeV neutrons into NE111 plastic scintillator material. For those events in which a proton is hit first the distribution of E_p against the time-of-flight of the scattered neutron to the second proton hit is shown on the left. The right hand figure shows the time-of-flight distribution. The fraction of events with $E_p > 200\mathrm{keV}$ and time-of-flight $>$ 0.4 ns is estimated to be 70%. Combined with the 27% events in which no carbon nuclei are hit an overall efficiency of 19% results.

4 Application

The application of the detector could be the standoff imaging, e.g. at border crossings, of hidden sources emitting fast neutrons, in particular of the fissile materials plutonium and uranium. The imaging of hidden sources of fast neutrons can fill a security gap that now exists, especially when used in combination with existing detection systems such as portal radiation monitors.

At a distance of 25 m, two times the length of a 40 ft sea container, the count rate of 1 kg WGP in the detector cube is about $\frac{6\times10^4}{4\pi 2500^2} \times 100\ \mathrm{cm}^2 = 0.07$ n/s. The rate of background neutrons which have a direction within the angular resolution of the detector can be estimated to be: $\frac{0.01\times100\ \mathrm{cm}^2}{128} = 0.008$ n/s; 10 times below the WGP count rate. In 5 minutes 20 WGP counts can be registered at 25 m distance on a 2 count background.

A specific application is the monitoring of sea containers that are stored on a so called stack in the harbor of Rotterdam. On an area of $50 \times 50\mathrm{m}^2$ more than 200 40 ft containers can be stacked that ideally can be scanned in a few minutes. An additional application may be to monitor incoming barges with containers before they get unloaded.

References

[1] (2002) The ABC news nuclear smuggling experiment. [Online]. Available: http://www.nrdc.org/nuclear/furanium.asp

[2] Andrew Clennell. (2002) Turkish police finds smuggled uranium. [Online]. Available: http://www.independent.co.uk/news/world/europe/turkish-police-find-smuggled-uranium-644020.html

[3] Lawrence Sheets. (2007) Georgia reports an attempt to smuggle uranium. [Online]. Available: http://www.npr.org/templates/story/story.php?storyId=7022263

[4] Tom Ricks and Dan Drezner and Stephen Walt and David Rothkopf and Marc Lynch. (2007) Smuggling uranium into the united states? a cakewalk. [Online]. Available: http://blog.foreignpolicy.com/posts/2007/03/20/smuggling_uranium_into_the_united_states_a_cakewalk

[5] M. S. Gordon, P. Goldhagen, K. P. Rodbell, T. H. Zabel, H. H. K. Tang, J. M. Clem, and P. Bailey, “Measurement of the flux and energy spectrum of cosmic-ray induced neutrons on the ground,” *IEEE Transactions on Nuclear Science*, vol. 51, December 2004.

[6] N.Nereson, “Fission neutron spectrum of pu239,” *Phys. Rev.*, vol. 88, pp. 823–824, 1952.

[7] P. E. Vanier *et al.*, “Design of a large-area fast neutron directional detector,” in *Conference Record*. IEEE Nucl. Sci. Symp., 2006, pp. 93–97.

[8] U. Bravar *et al.*, “Design and testing of a position-sensitive plastic scintillator detector for fast neutron imaging,” *IEEE Trans. Nucl. Sci.*, vol. 53, pp. 3894–3903, 2006.

[9] ——, “Atmospheric neutron measurements with the sontrac science model,” in *Conference Record*. IEEE Nucl. Sci. Symp., 2005, pp. 634–638.